Input evoked nonlinearities in silicon dendritic circuits

Yingxue Wang and Shih-Chii Liu
Institute of Neuroinformatics
University of Zürich and ETH Zürich
Winterthurerstrasse 190, CH-8057 Zürich, Switzerland
Email: yingxue,shih@ini.phys.ethz.ch

***Abstract*— Most VLSI spiking network implementations are constructed using point neurons. However, neurons with extended dendritic structures might offer additional computational advantages. Experimental evidence suggests that dendritic compartments could be considered as independent and parallel computational units. Depending on the synaptic input patterns, the dendritic integration could be either linear or nonlinear. We show the influence of spatio-temporal input patterns on the evoked dendritic integration in an aVLSI neuron chip with programmable dendritic compartments.**

I. Introduction

Pyramidal cells in neocortex and hippocampus have highly complicated dendritic structures, but the computational contribution of the dendritic tree in neuronal processing is still elusive. Experimental evidence suggests that individual dendritic branches can be considered as independent computational units, and NMDA channels located within the branches potentially allow either linear or nonlinear computation depending on the input s spatio-temporal pattern [1]–[6]. This evidence supports the two-layer model from Poirazi and colleagues [7], [8], which suggests that pyramidal cells first process their synaptic inputs within the individual dendritic compartments following a sigmoidal function before these signals are linear integrated at the soma. In contrast with the widely used point-neuron model, this two-layer model adds to the richness of neuron-level computation.

Most aVLSI spiking network implementations at present are constructed using point neurons. A few systems have included the passive cable circuit model of the dendrite [9], specifically by implementing the dendritic resistance using switched-capacitor circuits [10], [11]. Some researchers have also incorporated active channels into VLSI dendritic compartments [12], [13], and showed their use for the propagation of dendritic spikes [13]. However, the impact of the synaptic input pattern on the functionality of neurons with a dendritic tree has not been investigated. Physiological results suggest that temporally asynchronous and spatially distributed inputs evoke linear integration in the dendritic tree; while temporally synchronous and spatially clustered inputs evoke nonlinear integration [14]. To study this intriguing multi-functional device, we constructed an aVLSI neuron with a reconfigurable dendritic architecture. This architecture includes both individual computational units and spatial filtering.

In this paper, we show the impact of different spatio-temporal input patterns on the functionality of the neuron. This paper is structured as follows: In section II we introduce the aVLSI dendritic architecture; in section III we characterize the dendritic responses due to the nonlinearity of NMDA synapses; and in section IV, we show dendritic responses for different spatio-temporal patterns before we present concluding remarks.

II. Dendritic architecture

The silicon neuron circuit is composed of 9 dendritic compartments and 1 soma compartment (Fig. 1). Each dendritic compartment is an independent computational unit. This unit includes a nonlinear subunit which is capable of producing linear/nonlinear response according to the input pattern; a voltage-dependent dendritic spike-generating circuit; and a dendritic cable circuit that allows the interconnection between different compartments. The nonlinear subunit has 2 AMPA synapses, 2 AMPA+NMDA synapses, and 2 GABA synapses. The connections between compartments are fully programmable in both directions to create different dendritic architectures. The somatic spike can also be propagated back along the dendritic tree to the different compartments.

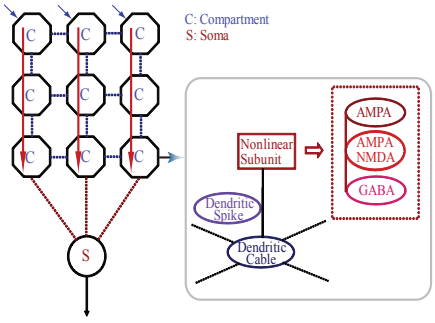

Fig. 1. Dendritic architecture. The neuron consists of 9 dendritic compartments (C) and 1 soma compartment (S), the dotted lines indicates the bidirectional programmable dendritic pathways. The solid red arrows in the figure show the programmed configuration for the experiments in Section III. The blue arrows indicate the stimulated compartments in those experiments. The right subfigure shows the components within each compartment. Layout size of each dendritic compartment is 87.8 μm by 231.1 μm.

The simplified circuitry is shown in Fig. 2. The circuit was fabricated in a 4-metal 2-poly 0.35 μm CMOS process. The

978-1-4244-3828-0/09/$25.00 ©2009 IEEE

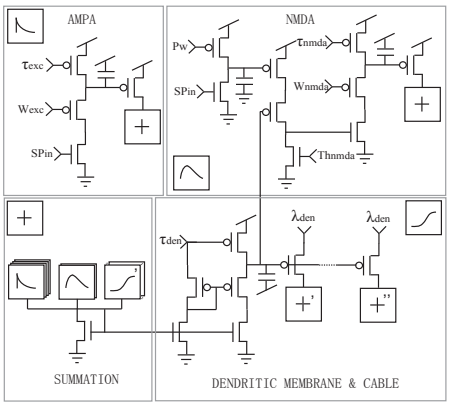

Fig. 2. Simplified schematics of the synaptic circuits in each compartment. The top left schematic shows the circuit for AMPA synapse, which is modeled as a low-pass filter (LPF). The top right schematic shows the NMDA synapse, which has a relatively long time constant and is sensitive to both the local dendritic membrane potential and the presynaptic stimulation. The bottom left schematic shows the circuit for the summation of currents from the individual synapses and neighboring compartments. The bottom right schematic shows the circuit for the integration of the currents on the dendritic membrane and the conveyance of this integrated current to neighboring compartments. The synapse and dendritic membrane circuits are based on the LFP circuits described in [12]. The biases are named in the following way: τ stands for time constant, W for synaptic weight, Th for threshold, Pw for pulse width, $SPin$ for synaptic spike input. In this paper, the time constants are set to τ_{ampa} = 0.6ms, τ_{nmda} = 15ms, τ_{den} = 3.8ms, τ_{soma} = 23.1ms, the dendritic spatial constant λ_{den} = 2.5 fold/compartment, the NMDA threshold V_{Thnmda} = 0.266V, and the soma threshold is 0.345V.

dendritic spike-generating circuit and GABA synapses are not discussed in this paper.

III. Temporal Processing

As mentioned above, the nonlinearity of the dendritic integration can be triggered by temporally synchronous synaptic input patterns. The nonlinearity we discuss in this paper is due to the NMDA channels. The state of these channels are controlled not only by the presence or absence of the agonist (e.g. glutamate), but also by the postsynaptic dendritic membrane potential. Hence, they play an important role in coincidence detection, and provide the superlinear influx current when the compartment receives temporally synchronous input [1], [2].

For the experiments in this section, we configured the chip so that it has 3 dendritic branches with 3 compartments each (see Fig. 1). Only the left branch is connected to the soma. Each of the 4 excitatory synapses (2 AMPA and 2 AMPA+NMDA synapses) in the top compartment of each branch is stimulated with a 20Hz regular spike train for 2s (indicated by the blue arrows in Fig. 1).The temporal offset, dt, between activated synaptic inputs varies as a parameter of the degree of synchrony.

A. Linear vs nonlinear response

To demonstrate the superlinear response contributed by the NMDA channels, we stimulate the top compartments with highly synchronous inputs, where dt = 1ms (1st row of Fig. 3). To illustrate the change in the soma response due to this nonlinearity, the NMDA channels are first blocked (shut off), and the linear integrated responses are recorded from each compartment (2nd to 5th row of Fig. 3). The highly synchronous inputs evoke sharp excitatory postsynaptic potentials (EPSPs) at the top compartments, but the signals degrade very fast in the direction of propagation. Since we use current mode membrane circuits, the membrane potentials or EPSPs are represented by current in *nA*. When we unblock (turn on) the NMDA channels, the sharp linear responses of the AMPA synapses activate the NMDA channels of the top compartments, leading to superlinear amplification (Fig. 4). The long time constant of the NMDA synapses (15ms), accounts for the slow EPSP component in the responses. The slow signals can propagate more effectively along the passive dendrite, thus eliciting much stronger somatic response (compare bottom rows of Fig. 3 and Fig. 4). For direct comparison of the membrane depolarization, somatic spikes are abolished in both cases.

Despite the circuit mismatch that leads to the variance in the linear EPSP response across the branches (2nd row of Fig. 3), the temporally synchronous input can trigger the nonlinearity in every compartment. This implies that the synchronous input pattern is more likely to activate the nonlinear response in the compartment.

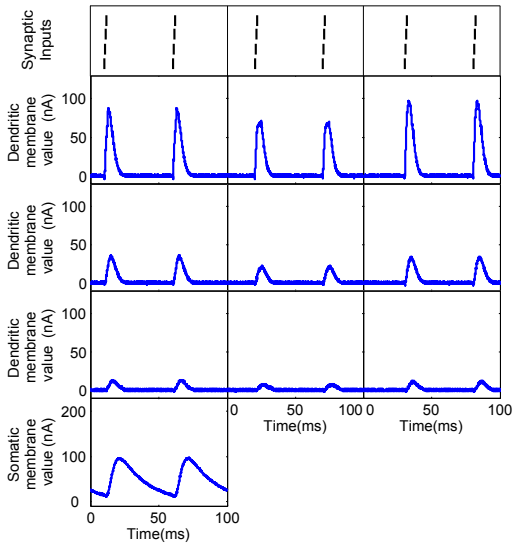

Fig. 3. EPSP responses of the compartments of each of the 3 dendritic branches (columnwise) when the NMDA channels are blocked (turned off). Each row shows the corresponding compartment for each of the 3 branches. Each column shows the effect of spatial smoothing along the 3 compartments of one branch. The bottom row shows the somatic EPSP evoked by the inputs from the left branch. The measured somatic response is amplified by a gain factor in the circuit.

B. Relationship between input synchrony and activation of nonlinearity

To quantify the relationship between the input temporal synchrony and the compartment function, we vary the input temporal offset dt from 0.5ms to 10ms, and record the peak EPSP of the top compartment of each dendritic branch and the soma both in the absence and presence of NMDA

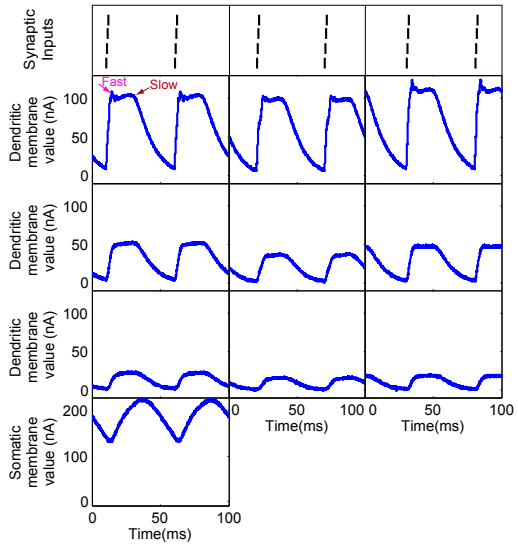

Fig. 4. EPSP responses of the compartments of each of the 3 dendritic branches (columnwise) when the NMDA channels are unblocked (turned on). The experimental setup is the same as in Fig. 3 except that the NMDA synapses are now activated by the temporally synchronous input. The NMDA response evokes the superlinear response within the stimulated compartments.

channels. The peak EPSP in the input-driven compartments is superlinear (Fig. 5 solid curves) across three branches when dt $\leq$1.5ms, in spite of mismatch. For dt $\leq$1ms, the peak corresponds approximately to the peak of the fast component in the response (indicated by the pink arrow in the 2nd row of Fig. 4) which is generated mainly by the strongly correlated AMPA responses. With increasing dt, NMDA influx current dominates the response, and the peak shifts toward the slow component relatively independent of the synaptic inputs (indicated by the red arrow in the 2nd row of Fig. 4). From dt $\geq$4.5ms on, the compartment response becomes linear for all branches. Then there is no difference between responses with NMDA channels blocked (Fig. 5 dashed curves) and unblocked (Fig. 5 solid curves).

As comparison, the dependence of the peak somatic EPSP on dt clearly follows a sigmoidal-like function (Fig. 6). Since the fast component in the response decays faster than the slow one along the spatial propagation, the amplification of the somatic response for small temporal offsets dt is due to the input-specific activation of the nonlinearity function in the compartment. With dt $>$ 2.5ms, the response returns to the linear case.

IV. Spatio-temporal processing

We bring together the results in Section III to illustrate the spatio-temporal interaction of the whole dendritic structure. We first programmed a random architecture for the dendritic tree, following the red lines in Fig. 7. We assigned a group of 4 inputs with a regular 20Hz rate to different spatial locations of the dendritic tree. In addition, the inputs have different temporal relations.

We show two cases of how a spatio-temporal input pattern evokes a different functionality of the dendritic tree. In the

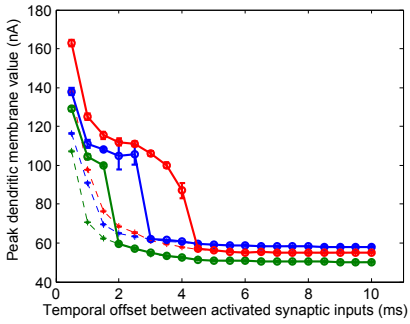

Fig. 5. The curves show the peak dendritic responses (current) from the top compartments of the 3 dendritic branches in response to 4 inputs with different input temporal offsets, dt. Blue (Left branch); Green (Middle branch); Red (Right branch). The mean and standard deviation of these measurements obtained over 10 trials are shown in these curves. The peak dendritic values for dt $\leq$1ms is due to the the peak of the fast response generated by the AMPA synapses. The responses in the absence (dashed curves) and presence (solid curves) of NMDA channels for these 3 compartments show that temporally synchronous inputs triggers the nonlinear function of the compartment, while temporally asynchronous inputs produce linear response.

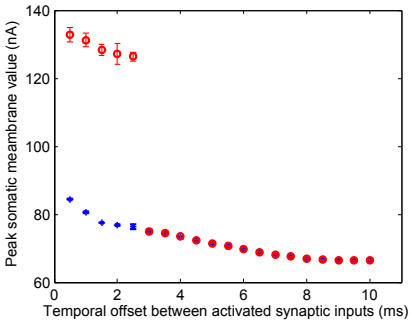

Fig. 6. Peak somatic responses (current) for the same experiment in Fig. 5. The mean and standard deviation over 10 trials are shown. The soma is connected to the left dendritic branch. The blue crosses and red circles correspond to the cases in the absence and presence of NMDA channels respectively. The measured somatic responses is amplified by a fixed gain over the actual responses.

first case, the inputs are temporally asynchronous (temporal offset between different inputs is dt=10ms) and spatially distributed (inputs go to different compartments). The membrane responses of all compartments are shown in Fig. 7, along with the location and temporal ordering of the inputs. In this case, individual compartments linearly integrate their inputs leading to a linear spatio-temporal response at the soma (last row of Fig. 7).

In the second case, the inputs are temporally synchronous and spatially clustered (2 inputs per compartment). This spatio-temporal input pattern triggers the nonlinear computation within the two stimulated compartments (C1 and C3), and leads to a somatic spike (last row of Fig. 8).

In summary, the results show that because of the NMDA induced nonlinear response, the dendritic structure is able to distinguish between two different spatio-temporal input patterns which could correspond to two distinct network states [14].

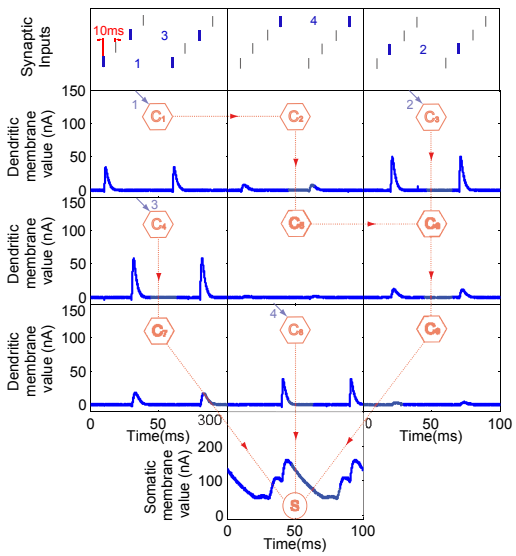

Fig. 7. Membrane response of each dendritic and somatic compartment for temporally asynchronous and spatially distributed inputs (The time diagram is shown in the 1st row. Inputs to each column are highlighted in blue). The programmed dendritic tree is superimposed on the top of the response curves. The red line indicates the existence of a connection between the corresponding compartments, and the red arrow specifies the direction of signal flow. The blue arrow at a compartment symbol C marks an input to that compartment and the associated number indicates the temporal order of the input. The smallest temporal offset between different synaptic inputs is 10ms. This spatio-temporal pattern evokes linear integration in the dendritic structure.

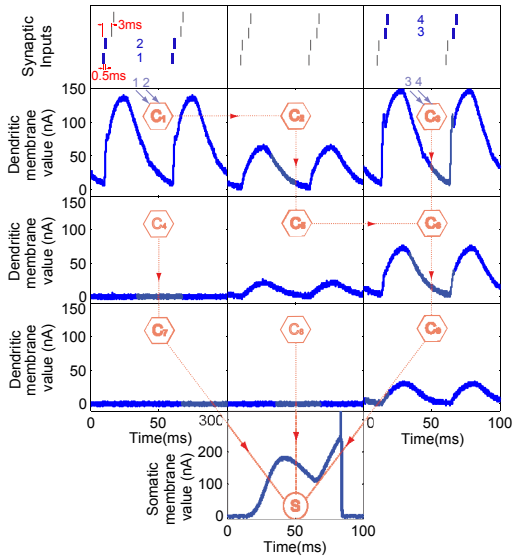

Fig. 8. Membrane response of each dendritic and somatic compartment for temporally synchronous and spatially clustered inputs. In this case, the temporal offset between the inputs to the same compartment is 0.5ms, and the offset between inputs to different compartments is 3ms. The NMDA channels within input compartments C1 and C3 are activated, leading to a nonlinear integration of inputs at the dendrite. A somatic spike is generated in response to this input pattern.

V. Conclusion

The reason for the existence of a dendritic architecture could be as simple as a way for a neuron to collect inputs from spatially distant layers. However, the dendritic architecture is ideal for parallel local computations on a set of inputs before the summation at the soma. In this work, we show results that illustrate possible computational advantages of this local computation on the dendritic tree. The results show that the dendritic tree can respond differently to different spatio-temporal input patterns. Temporally synchronous and spatially clustered input can evoke nonlinear integration while temporally asynchronous and spatially distributed inputs will evoke primarily linear dendritic integration. These differences imply that dendrites can have multiple input-activated functions under distinct network states.

VI. Acknowledgments

We acknowledge Rodney Douglas for multiple discussions on dendritic functions. We also acknowledge members of the Institute of Neuroinformatics, particularly Adrian Whatley, who was involved in the development of the PCI-AER board, of its drivers, and software library components, and Dylan Muir who developed the spike tool box. This work was supported by the ETH Research Grant TH-20/04-2.

References

[1] J. Schiller, G. Major, H. J. Koester, and Y. Schiller, "Nmda spikes in basal dendrites of cortical pyramidal neurons," *Nature*, vol. 404, no. 6775, pp. 285–289, 2000.

[2] D. Wei, Y. A. Mei, A. Bagal, J. Kao, S. Thompson, and C. Tang, "Compartmentalized and binary behavior of terminal dendrites in hippocampal pyramidal neurons," *Science*, vol. 293, no. 5538, pp. 2272–2275, 2001.

[3] A. Polsky, B. Mel, and J. Schiller, "Computational subunits in thin dendrites of pyramidal cells," *Nature Neuroscience*, vol. 7, no. 6, pp. 621–627, Jun 2004.

[4] S. Gasparini, M. Migliore, and J. Magee, "On the initiation and propagation of dendritic spikes in CA1 pyramidal neurons," *Journal of Neuroscience*, vol. 24, no. 49, pp. 11 046–11 056, 2004.

[5] A. Losonczy and J. Magee, "Integrative properties of radial oblique dendrites in hippocampal CA1 pyramidal neurons," *Neuron*, vol. 50, no. 2, pp. 291–307, 2006.

[6] G. Ariav, A. Polsky, and J. Schiller, "Submillisecond precision of the input-output transformation function mediated by fast sodium dendritic spikes in basal dendrites of CA1 pyramidal neurons," *Journal of Neuroscience*, vol. 23, no. 21, pp. 7750–7758, 2003.

[7] P. Poirazi, T. Brannon, and B. Mel, "Arithmetic of subthreshold synaptic summation in a model CA1 pyramidal cell," *Neuron*, vol. 37, no. 6, pp. 977–987, 2003.

[8] P. Poirazi, T. Brannon, and B. Mel, "Pyramidal neuron as two-layer neural network," *Neuron*, vol. 37, no. 6, pp. 989–999, 2003.

[9] W. Rall, "Theoretical significance of dendritic trees for neuronal input-output relations," in *Neural Theory and Modeling*, R. F. Reiss, Ed. Stanford, CA: Stanford Univ. Press, pp. 73–97, 1964.

[10] C. Rasche and R. Hahnloser, "Silicon synaptic depression," *Biological Cybernetics*, vol. 84, no. 1, pp. 57–62, 2001.

[11] J. G. Elias and D. P. M. Northmore, "Building silicon nervous systems with dendritic tree neuromorphs," in *Pulsed Neural Networks*, W. Maass and C. M. Bishop, Eds. Boston, MA: MIT Press, ch. 5, pp. 135–156, iSBN 0-262-13350-4, 1999.

[12] J. V. Arthur and K. A. Boahen, "Recurrently connected silicon neurons with active dendrites for one-shot learning," *International Joint Conference on Neural Networks (IJCNN)*, pp. 1699–1704, 2004.

[13] E. Farquhar, D. Abramson, and P. Hasler, "A reconfigurable bidirectional active 2 dimensional dendrite model," *Proceedings of the 2004 IEEE International Symposium on Circuits and Systems*, vol. V, pp. 313–316, 2004.

[14] S. Gasparini and J. Magee, "State-dependent dendritic computation in hippocampal CA1 pyramidal neurons," *Journal of Neuroscience*, vol. 26, no. 7, pp. 2088–2100, 2006.